Proceedings of International Collaboration on Advanced Neutron Sources (ICANS-VII), 1983 September 13-16
Atomic Energy of Canada Limited, Report AECL-8488

RECENT TARGET DESIGN CALCULATIONS AT KFA

P. Cloth, D. Filges, R.D. Neef, H. Schaal

Institut für Reaktorentwicklung, Kernforschungsanlage Jülich GmbH
Postfach 1913, D-5170 Jülich, Germany

ABSTRACT

The target design calculations described here were performed for the two proposed proton beam energies (350 MeV and 1100 MeV) and different target material mixtures as tungsten, lead and uranium. The results for some important nuclear parameters as neutorn production, neutron fluxes and energy deposition were discussed. Preliminary calculations for the high energy source shielding and "grooved" moderator design were also shown.

INTRODUCTION

The recent target design calculations made by KFA are mainly performed for comparisons of nuclear parameters of the SNQ target station at the two forseen proton beam energies of 350 and 1100 MeV. One aim of these calculations was to optimize the targets for different materials and beam energies.

EVALUATIONS FOR PROTON BEAM ENERGIES OF 350 MEV VS 1100 MEV

All calculations were performed with HETC/KFA-1 /1/ and based on the 3-D target model described in detail in Ref. /2/. The main parameters for the calculations are shown in Table I.

Table I Parameters for Calculations

Beam Parameters:	
- kinetic energy:	350 MeV/1100 MeV
- particles:	protons
- average current:	5 mA
- pulse current:	200 mA
- pulse width:	0.25 ms
- pulse frequency:	100 s^{-1}
- beam profiles:	gaussian 4 cm FWHM truncated at radius = 4 cm
Targets:	
- geometry:	rotating "wheel"
- materials:	U_{dep}(0.2 nat% ^{235}U)-, Pb-, W-H_2O/Al mixtures*, and solid W
- cladding/structur:	aluminium
- coolant:	H_2O
Moderators:	H_2O/D_2O
Shielding-Material:	cast iron and concrete

*mixture: heavy material 76.5 %
cladding 7.0 %
coolant 16.5 %

1. Neutron production, neutron fluxes in H_2O moderator and energy deposition for different target materials (W, Pb, U_{dep})

In table II the neutron yields (< 15 MeV) per proton in the target are compared for proton beam energies of 350 and 1100 MeV and for different target compositions as described in table I. Additionally in table III the particle production for the uranium case is given.

Table II Neutron Yield per Proton in Target-Region

	(n/p < 15 MeV)		
Material	350 MeV	1100 MeV	ratio 1100/350
U_{dep}-H_2O-Al	5.15	30.12	5.8
Pb-H_2O-Al	3.43	19.53	5.7
W-H_2O-Al	4.16	21.3	5.12
W_{solid}	4.49	23.3	5.19

Table III Comparison of Particle Production for U_{dep}-Targets

	350 MeV	1100 MeV	ratio 1100/350
Neutrons produced per proton in the system			
< 15 MeV	5.87	35.6	6.1
Neutron yield per proton in target			
< 15 MeV	5.15	30.12	5.8
> 15 MeV	0.51	3.7	2.3
Charged particle yields per proton			
protons	0.44	4.0	9.0
pions	1.7×10^{-3}	2.8×10^{-1}	170
(neutral pions)	2.0×10^{-3}	1.9×10^{-1}	95

A comparison of thermal neutron fluxes (10^{-5} - 0.41 eV) in the fast moderator (size: length x height x width 20x12x15 cm^3) is given in table IV. The given thermal fluxes are the average omnidirectional thermal fluxes within that position of the moderator defined by the total moderator length of 20 cm (along the beam direction), the total moderator height of 12 cm (direction perpendicular to beam tube axis), and the central 5 cm region of the 15 cm moderator width (direction along beam tube axis). For details see Ref. /2/. In all calculations the moderator had the same positions and size, therefore none of these data were optimized for the special target composition and beam energy.

Table IV Thermal Neutron Fluxes in Fast Moderator* (thermal energy 10^{-5} - 0.41 eV)

Target	Φ_{th} (a) ($n/cm^{-2}\ s^{-1}$/proton) 350 MeV	1100 MeV	Φ_{th} (b) ($n/cm^{-2}\ s^{-1}$) 350 MeV	1100 MeV
U_{dep}-H_2O-Al	4.9×10^{-3}	2.65×10^{-2}	1.5×10^{14}	8.3×10^{14}
Pb-H_2O-Al	2.9×10^{-3}	1.6×10^{-2}	0.9×10^{14}	5.0×10^{14}
W-H_2O-Al	3.5×10^{-3}	1.8×10^{-2}	1.1×10^{14}	5.6×10^{14}
W-solid	3.9×10^{-3}	2.0×10^{-2}	1.2×10^{14}	6.2×10^{14}

(a) neutron fluence per beam proton
(b) average neutron flux for I = 5 mA
*same system for all calculations, not optimized

The depth distributions of the calculated energy deposition inside the target "mixture" (i.e. the homogenized region of the target wheel) are shown in Figure 1. The deposition for 350 MeV beam energy is predominately due to ionization by primary protons and secondary protons for all target materials. However, for 1100 MeV beam energy in case of uranium as target material only about 30 % of the energy deposition is caused by primary and secondary protons, whereas the rest comes from high energy fission and low energy neutron induced fission. From Figure 1 it can be seen that cooling problems for 350 MeV beam energy may arise from Bragg-peak energy deposition at the end of the proton range. In table V the peak energy deposition corresponding to a single pulse for different target materials and 350 MeV and 1100 MeV beam energy is given. In table VI the total deposition in the target wheel for an average proton beam current of I = 5 mA for both energies and all target materials is compared. If the proton beam energy is increased to 1100 MeV the energy deposition in the lead is enlarged by a factor of 2 whereas for the uranium target the deposition increases by factor of about 5.

Table V Peak Energy Deposition for U_{dep}, Pb, W as Target Material

Target	350 MeV(1) MeV/cm^3-proton	Peak Deposition kJ/cm^3 per pulse**
U_{dep}-H_2O-Al	4.3	0.215
Pb-H_2O-Al	3.63	0.18
W-H_2O-Al	4.5	0.225
W-solid	4.36	0.218

Target	1100 MeV (2) MeV/cm^3-proton	Peak Deposition kJ/cm^3 per pulse**
U_{dep}-H_2O-Al	3.0	0.15
Pb-H_2O-Al	1.2	0.06
W-H_2O-Al	-	-
W-solid	-	-

** pulse current I = 200 mA, pulse width 0.25 ms
pulse frequency 100 s^{-1}
(1) for radial intervall about beam axis r=1.0 cm
(2) for radial intervall about beam axis r=1.5 cm

Table VI Comparison of Heating for U_{dep}, Pb, W as Target Material*

Deposition in Target (MeV)	U_{dep}	350 MeV Pb	W_{mix}	W
> 15 MeV	366	292	288	287
< 15 MeV	210	6	30	10
Total Deposition MeV/P	576	298	318	297
Total Deposition in MW for I=5 mA	2.88	1.49	1.59	1.48

Deposition in Target (MeV)	U_{dep}	1100 MeV Pb	W_{mix}	W
> 15 MeV	973	542	-	-
< 15 MeV	1515	29	-	-
Total Deposition MeV/P	2488	571	-	-
Total Deposition in MW for I=5 mA	12.44	2.86	-	-

*Depth of systems not optimized

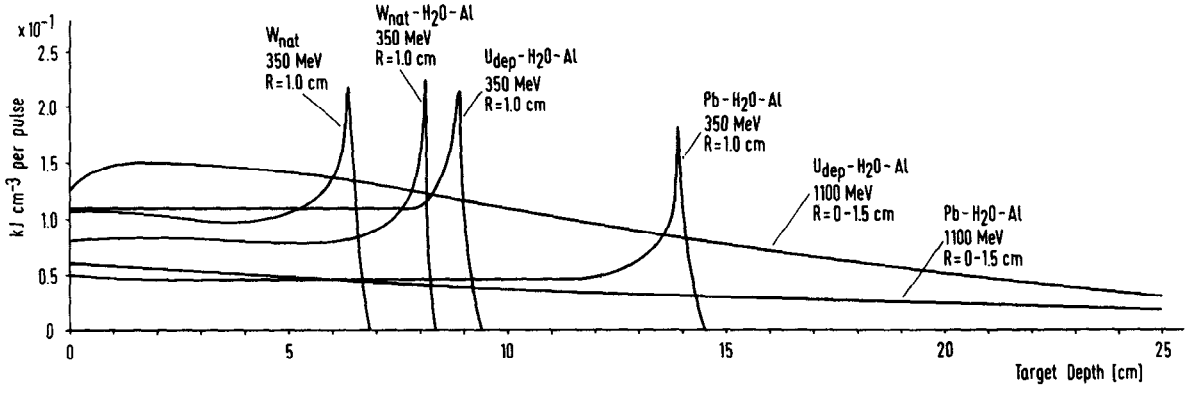

Figure 1 Energy deposition inside target wheel (axial)

2. High Energy Source Shielding

The calculations were done in a coupled procedure with the Monte Carlo code HETC/KFA-1 and the one-dimensional transport code ANISN /3/. For the HETC calculations the target area was surrounded by a sphere of 5 m thickness, consisting of cast iron. HETC calculated the angular dependent fast neutron flux (E_n > 50 MeV) at spherical shells around the target center (see fig. 2) thus generating a shell source for ANISN. For the ANISN calculations a sphere with 4 m of cast iron and 1 m of concrete was supposed. The cross section data were taken from LANL-library. ANISN calculated the neutron flux and the dose rate inside the shield.

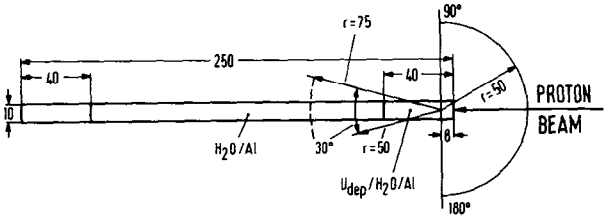

Figure 2 Simulation of high energy source for 1-D ANISN shielding calculations

The first question was, whether it would be useful to build different shieldings for 350 MeV and for 1100 MeV proton beam energy. Fig. 3 shows the dose rate vs. sphere radius for both cases. The curves have different intensities, but the same shape. So to get same dose rate at the outer edge of the shield, the dose rate curve for E_p=1100 MeV has to be extrapolated as shown in Fig. 4. Then the difference ΔL=80 cm means, that the cases 350 MeV and 1100 MeV have to be different in 80 cm thickness of iron only. So it does not seem to be reasonable to build different shields.

The second question was, whether the shield thickness should be the same in forward as in backward direction for 1100 MeV beam energy. A comparison of angular dependent fast neutron yields (from HETC calculations) lead to a dose rate ratio forward to backward (for constant thickness of the shield) of about 20, but coupling calculations give a ratio of about 1000. The reason for this difference lies in the fact, that the energy spectrum (see Fig. 5) in the forward direction is much harder than in the backward direction and that the angular shape in backward direction is more isotropic than in forward direction. So it can be stated that different shield thicknesses in forward and backward direction should be taken into account. Detailed studies are planned.

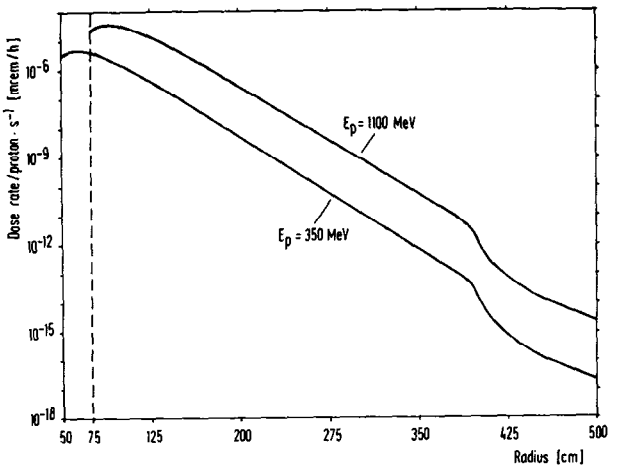

Figure 3 Coupled dose rate calculations (HETC/ANISN) in forward direction

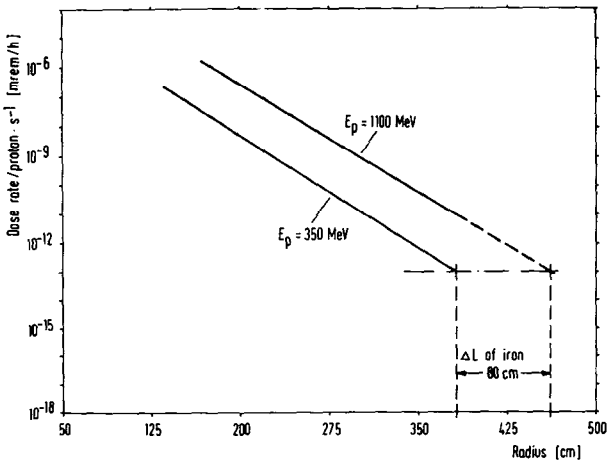

Figure 4 Determination of additional shielding thickness comparing 350 MeV and 1100 MeV proton beams

STUDIES FOR TARGET OPTIMIZATION

1. Target Depths and Fast Moderator Position for 350 and 1100 MeV Proton Beam Energy

To determine optimal target depths dependent on the different target material compositions the following criteria have to be taken into account

- proton range
- spatial dependent neutron production in the target
- escape distribution on the surface of the target
- spatial dependent energy deposition
- material saving
- minimum of radioactive inventory

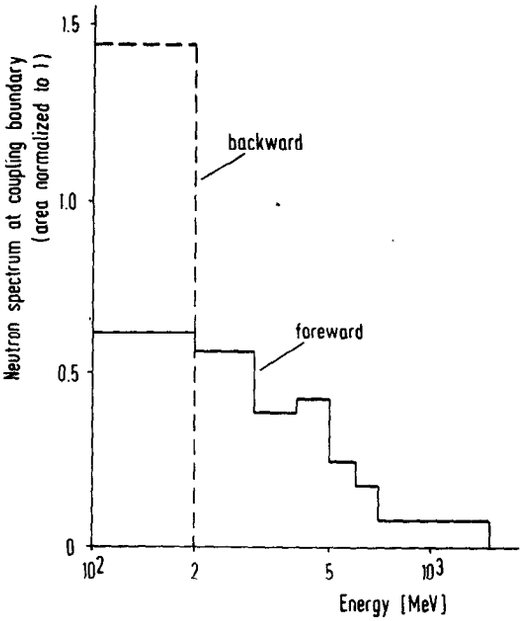

Figure 5 Neutron spectra for 1100 MeV proton beam energy for uranium target in forward and backward direction (coupling surface R=75 cm see Fig.2)

The proton ranges for the relevant targets are given in table VII.

Table VII Proton Ranges and Bragg Peak Position

Target	Bragg Peak Position 350 MeV (cm)	Proton Range (cm) 350 MeV	1100 MeV
U_{dep}-H_2O-Al	8.8	9.0	48.3
Pb-H_2O-Al	13.8	14.0	75.9
W-H_2O-Al	8.12	8.25	44.4
W-solid	6.3	6.75	40.0

In Figure 6 the spatial dependent neutron production in the target for 350 MeV beam energy is plotted. From these calculations the cummulative production rates were determined and are shown in Fig. 7. To avoid the high energy deposition in the "Bragg"-peak area (see Fig. 1) the target depth should not include the "Bragg"-peak position. This condition is fullfilled if one cuts the cummulative curve of neutron production at 85%. In the 1100 MeV case, the optimal target depth was estimated from the cummulative escape distributions of neutrons in proton beam direction. This was done because the proton range is very large compared to range of the 350 MeV protons therefore the escape distribution of neutrons determines the depth of the target system. In table VIII the optimal target depths for both energies are given.

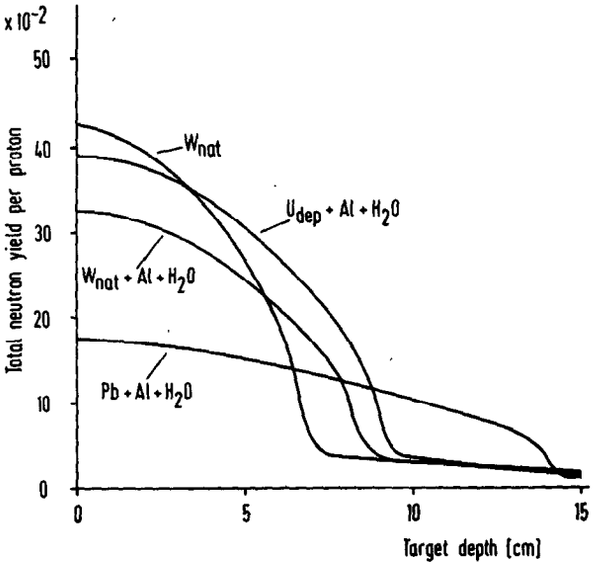

Figure 6 Spatial dependent neutron production rates in target wheel (350 MeV beam energy)

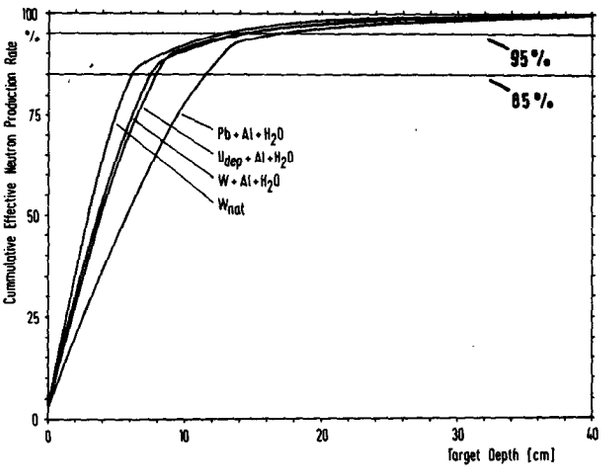

Figure 7 Cummulative effective neutron production rate vs. target depth (350 MeV beam energy)

The position of the fast moderator for 350 MeV and 1100 MeV proton energy depends on the spatial neutron flux or neutron current distributions. The center of the moderator should be located below the maximum of the escape distribution or flux distribution of the targets. In Figures 8 - 10 the distributions are shown. From these distributions the moderator positions for 350 MeV and 1100 MeV beam energy and different target mixtures are determined and given in Table IX.

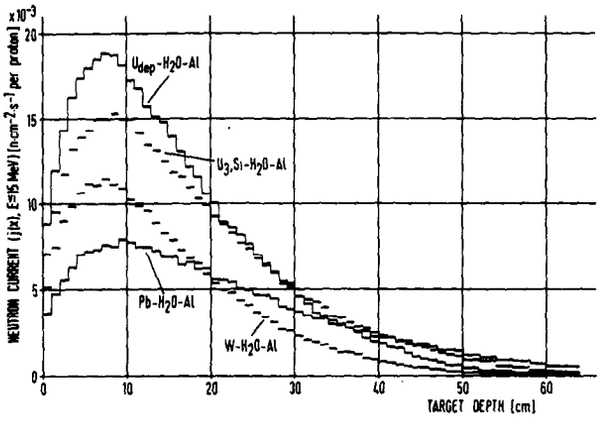

Figure 8 Escape distributions for different target mixtures vs. target depth (1100 MeV beam energy)

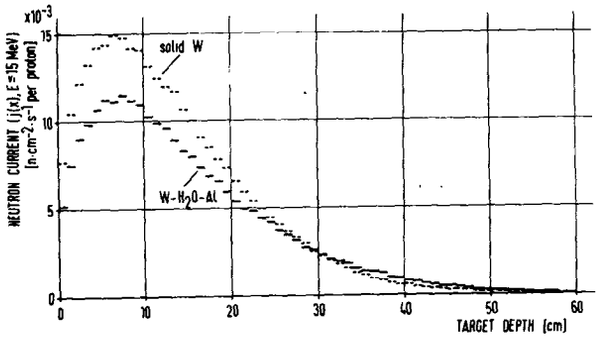

Figure 9 Escape distributions for W-mixtures and W-solid targets vs. target depth (1100 MeV beam energy)

Table VIII Target Depth for 350 MeV and 1100 MeV proton beam energy

Target	Target Depth (cm) 350 MeV 85% cummulative neutron production	1100 MeV 95% cummulative neutron escape distribution
U_{dep}-H_2O-Al	8.0	36.0
Pb-H_2O-Al	12.0 (13.0 for 90%)	68.5
W-H_2O-Al	7.75	36.0
W-solid	6.0	31

Table IX Moderator Positions for 350 MeV and 1100 MeV Proton Energy

Target	350 MeV	1100 MeV
	Peak Position=Center of Moderator (cm)	
U_{dep}-H_2O-Al	4.0 - 5.0	7.5 - 8.5
Pb-H_2O-Al	6.0	8.0 - 11.0
W-H_2O-Al	4.0	7.0 - 8.0
W-solid	3.0 - 4.0	6.5 - 7.5

2. Moderators

Fast Moderators have to be optimized in their geometrical dimensions as well as in their structural material components. Experiments show in special cases that "grooved" moderators give higher detector responses for thermal neutrons than solid moderators. To study this phenomenology a special fast running 3-D geometry model for HETC/MORSE Monte Carlo calculations was developed /4/. The advantage of this geometry model is easy parameter variation for overall size of the moderator and description of grooves and fins including structure and moderator material. Point detector estimation of escaping neutron fluxes and currents in energy time and space with importance sampling is used. Some preliminary results to show possible gains for grooved moderators (24 grooves)

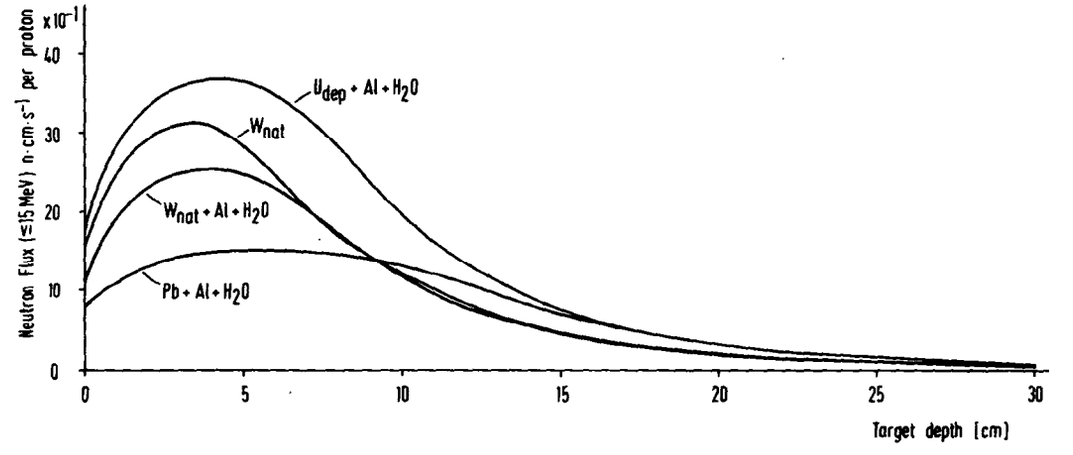

Figure 10 Neutron flux distributions for different target mixtures vs. target depth (350 MeV beam energy)

compared with solid moderators are shown in Figure 11. The study is in progress. Results will be published.

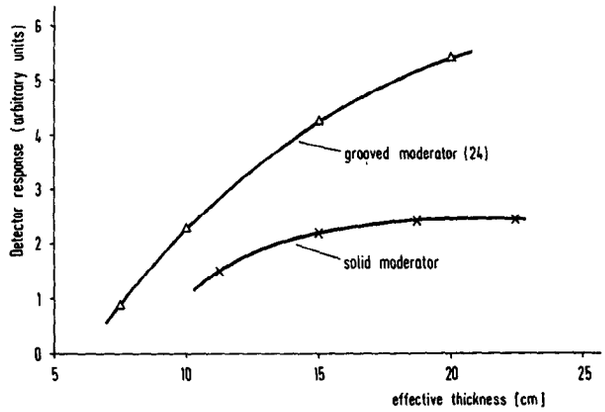

Figure 11 Comparison of detector responses (thermal energy 10^{-5} - 0.4 eV) for solid and grooved moderators of same overall size

Investigations on cold sources were started evaluating cross section for hydrogen (H_2) at 20° K for different mixtures of para- and orthohydrogen. The new cold source of KFA-DIDO research reactor has been designed with these data and is now under construction. Results should be available in about one year. Details of the data evaluation and the design will also be published.

REFERENCES

/1/ P. Cloth, D. Filges, G. Sterzenbach, T.W. Armstrong, B.L. Colborn
The KFA-Version of the High-Energy Transport Code HETC and the generalized Evaluation Code SIMPEL
KFA-Report Jül-Spez-196, March 1983

/2/ T.W. Armstrong, P. Cloth, D. Filges, R.D. Neef
Theoretical Target Physics Studies for the SNQ Spallation Neutron Source
KFA-Report Jül-Spez-120, July 1981

/3/ H. Schaal, M. Kloda, G. Sterzenbach
Internal Note, SNQ 3 J../BH 191082

/4/ To be published as KFA-Jül-Report

/5/ To be published as KFA-Jül-Report